2016 ERDKUNDE Vol. 70 · No. 1 · 69–82

HYDRO-CLIMATIC VARIABILITY IN SOUTHERN ECUADOR REFLECTED BY TREE-RING OXYGEN ISOTOPES

Franziska Volland, Darwin Pucha and Achim Bräuning

With 5 figures and 5 tables
Received 22 May 2015 · Accepted 18 January 2016

Summary: Variations of stable oxygen isotopes in tree-ring cellulose are a widely used proxy to reconstruct hydro-climate variability in tropical and subtropical regions. We present the first $\delta^{18}O$ chronology from annual tree rings in tropical *Cedrela montana* trees growing in the mountain rain forest of the Podocarpus National Park (PNP) in southern Ecuador. The more than a century long data record (1885–2011) comes from up to 15 individual trees (1980–2005) and represents the best-replicated isotope tree-ring chronology from the tropics. In comparison with tree-ring width, stable isotope variations show considerably higher correlations between individuals and thus represent a more reliable climate proxy in this very humid environment. High teleconnections to other stable isotope chronologies from the Amazon lowland indicate a high degree of consistency of regional hydro-climate variations. The PNP $\delta^{18}O$ record is correlated with seasonal precipitation (January to April, CRU TS 3.21), frequency of wet days, and cloud cover over the Andean Cordillera Real. Spatial correlations indicate that the El Niño-Southern Oscillation (ENSO) has strong impact on tree-ring $\delta^{18}O$ variations. Sea Surface Temperatures (SSTs) of the Niño 3.4 region and Niño 4 region, and the Oceanic Niño Index (ONI) show strong positive correlations with Cedrela oxygen isotope ratios, whereas the ENSO precipitation index correlates negatively. The Niño 3.4 and 4 SST influence is stronger after 1960 than before, indicating a shift in the influence of the Pacific Ocean on moisture variations in the Ecuadorian Andes. In the same period, the positive correlation with oxygen isotope signals from Andean glacier ice cores ($r=0.2$; $p<0.05$, 1894–1993) increased strongly ($r=0.51$; $p<0.01$, 1960–1993). In conclusion, stable oxygen isotope series from tropical tree species can help reconstruct variations in the hydroclimate of the Andean mountains and their surrounding areas.

Zusammenfassung: Für die Rekonstruktion hydrologischer Klimavariabilität in den Tropen und Subtropen sind stabile Sauerstoffisotope in der Zellulose von Jahrringen ein weit verbreiteter Klima-Proxy. Wir präsentieren die erste jährlich aufgelöste $\delta^{18}O$-Chronologie aus Jahrringen der tropischen Baumart *Cedrela montana* aus dem feuchten Bergregenwald Süd-Ecuadors (Podocarpus-Nationalpark (PNP)). Die vorliegende Zeitreihe umfasst eine Zeitspanne von 126 Jahren (1885–2011) und basiert auf bis zu 15 Einzelbäumen (1980–2005). Sie stellt damit die momentan besten belegte $\delta^{18}O$-Jahrring-Zeitreihe aus den immerfeuchten Tropen dar. Im Vergleich zur Jahrringbreite zeigen die stabilen Sauerstoffisotope deutlich höhere Zusammenhänge zwischen den einzelnen Individuen und stellen somit einen sehr zuverlässigen Klima-Proxy in tropisch-humiden Klimabedingungen dar. Hohe Telekonnektionen zu anderen regionalen $\delta^{18}O$-Chronologien (z.B. aus dem Amazonas-Tiefland) zeigen eine signifikante Ähnlichkeit und belegen eine hohe räumliche Repräsentativität. Die PNP $\delta^{18}O$ Messreihen korrelieren hoch signifikant mit verschiedenen Niederschlags-Monatsmitteln und saisonal gemittelten Niederschlagsreihen (z.B. für CRU TS 3.21 Januar bis April), der Frequenz von Feuchttagen und dem Bewölkungsgrad über der Cordillera Real der tropischen Anden. Räumliche Korrelationen zeigen einen hoch signifikanten negativen Zusammenhang zwischen dem El-Niño-Southern Oscillation Niederschlag-Index (ENSO prec.) und den $\delta^{18}O$ Jahrring-Werten. Die Meeresoberflächentemperaturen der Niño 3.4 und 4 Regionen und der Oceanic Niño Index (ONI) zeigen dagegen hohe positive Korrelationen mit den Cedrela-Sauerstoffisotopen-Verhältnissen. Allerdings nimmt der Einfluss der Meeresoberflächentemperaturen der Niño 3.4 und 4 Regionen ab 1960 stark zu, was auf einen höheren Einfluss des Pazifik auf das Feuchtigkeitsregime in den ecuadorianischen Anden deutet. Gleichzeitig nahm die signifikant positive Korrelation mit $\delta^{18}O$ Werten in andinen Eisbohrkernen von $r=0.2$ ($p<0.05$, 1894–1993) auf $r=0.51$ ($p<0.01$, 1960–1993) zu. Zeitreihen stabiler Sauerstoffisotope in Jahresringen tropischer Bäume können dazu beitragen, Schwankungen im Hydroklima der Andenregion zu entschlüsseln.

Keywords: Climate variability, oxygen isotopes, tropical mountain rain forest, Ecuador, *Cedrela montana*

1 Introduction

The perhumid ecosystem 'lower tropical mountain forest' in southern Ecuador is characterized by a high number of vascular plant species and belongs to the "hottest" hotspots of global biodiversity (Richter et al. 2013). Among the more than 280 native tree species, the broad-leaved deciduous species *Cedrela montana* is particularly well suited for dendroclimatological studies due to its distinct annually formed tree-rings that can be synchronized between individuals to calculate tree-ring chronologies (Bräuning et al. 2009; updated chronology unpub-

DOI: 10.3112/erdkunde.2016.01.05 ISSN 0014-0015 http://www.erdkunde.uni-bonn.de

lished). During recent years, numerous studies have documented the formation of annual tree rings in neotropical tree species (e.g. Schöngart et al. 2002; Worbes 2002; Bräuning et al. 2009; Rozendaal et al. 2010; Stahl et al. 2010; Volland-Voigt et al. 2011; Brienen et al. 2012; Soliz-Gamboa et al. 2012), using the wood parameters tree-ring width, and the variations of stable oxygen and carbon isotopes in wood ($\delta^{18}O$ and $\delta^{13}C$). Thus, tree-ring series with their high temporal resolution and dating accuracy have gained increasing importance as archives for (paleo-) climate investigations in tropical South America.

The availability of climate data for the Andean Cordillera Real is rather poor in spatial resolution and length of data series, thereby limiting our understanding of regional past climate variability. These circumstances underline the need of reliable paleoclimate proxies to reconstruct past climate variability and to better understand stable isotope fractionation processes in different archives, such as stable oxygen isotope ratios in precipitation (Villacis et al. 2008), soil water (Goller et al. 2005), and ice cores (Thompson et al. 2000; Vimeux et al. 2009). The first two types of records are often short-term and incomplete. In contrast, ice core data are sometimes very long, but current data is often missing (Thompson et al. 2013). Therefore, tree-ring oxygen isotope values are a promising tool for high resolution (annual) climate reconstructions for past centuries (Zuidema et al. 2013). For tropical South America, Ballantyne et al. (2011) and Brienen et al. (2012) presented the first studies about long-term and large-scale atmospheric processes and precipitation variability derived from tree-ring oxygen isotopes.

The variation of tree-ring $\delta^{18}O$ is determined (i) by the amount and isotopic composition of precipitation, (ii) by the enrichment of leaf water ^{18}O caused by transpiration, and (iii) by the ^{18}O fractionation processes during the biosynthesis of carbonyl oxygen and the post-photosynthetic isotope exchange during the formation of tree-ring cellulose (Sternberger and De Niro 1983; Sternberger et al. 1986; McCaroll and Loader 2004; Liu et al. 2014; Gessler et al. 2014; Treydte et al. 2014). Precipitation has a strong influence on tree-ring $\delta^{18}O$. Amount and isotopic composition of precipitation in the Andean mountains is in turn influenced by the origin of the moist air mass and by landscape topography (Sturm et al. 2007). Precipitation inflow from the Amazon Basin dominates the isotopic signal in ice cores from the South American Andes (Hoffmann et al. 2003), while Pacific sea surface temperature anomalies (Vuille et al. 2003), and the El Niño-Southern Oscillation (ENSO) phenomenon (Bradley et al. 2003) also influence the signal. During the air-mass-transport over land, heavy isotopes condense faster (Dansgaard 1964) and hence an air mass travelling further inland becomes increasingly depleted. The degree of depletion depends on increasing altitude, distance to the origin source, and intensive rainfall events (the so called "amount effect"). More depleted water vapour (more negative $\delta^{18}O$) occurs during wetter years compared to drier years, resulting in inter-annual variations of the isotope signal in high-resolution proxies.

Numerous studies have successfully reconstructed regional precipitation signals from tree-ring $\delta^{18}O$ series, e.g. in Thailand (Poussart and Schrag 2005) and Indonesia (Schollean et al. 2013). A number of studies also detected signals of El Niño-Southern Oscillation (ENSO) variability in tree-ring $\delta^{18}O$ series, e.g. in South-East Asia (Liu et al. 2014; Xu et al. 2011, 2013a, 2013b; Sano et al. 2012; Zhu et al. 2012) or South America (Brienen et al. 2012).

So far, however, no study has yet been conducted in the humid (annual precipitation > 2000 mm) mountain forest of the tropical Andes. In the present study we present the first results on climate signals derived from tree-ring oxygen isotopes in Ecuadorian Cedro (*Cedrela montana*). We hypothesized that tree-ring $\delta^{18}O$ series share a strong common signal between tree individuals, and therefore provide a strong environmental signal in a tree population. We tested if tree-ring $\delta^{18}O$ is correlated to climate parameters and other stable isotope proxies, including meteoric precipitation, sea surface temperatures, different ENSO indices, as well as $\delta^{18}O$ ice core records from the Andes, which share the same origin of moisture as our study area.

2 Study site, local climate and species

The study site "Reserva Biológica San Francisco" (RBSF 1800–3180 m a.s.l., 3.58°S, 79.04°W, Fig. 1) is located in the Rio San Francisco valley at the northern slope of the Podocarpus National Park (PNP) in southern Ecuador. The local vegetation can be classified as an evergreen montane forest (Balselv and Øllgaard 2002) or as lower montane rainforest (Homeier 2004).

Local climate data within a distance of 1 km from the sampling sites has been collected since 1998. In this data mean annual air temperature is 15.3 °C

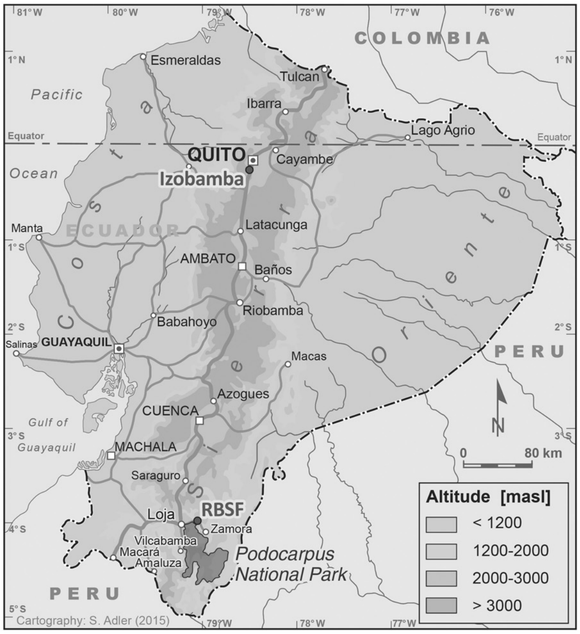

Fig. 1: Locations of the Podocarpus National Park (PNP) in southern Ecuador with study region Reserva Biológica de San Francisco (RBSF), and GNIP (Global Network of Isotopes in Precipitation) station Izobamba

and mean annual relative humidity amounts to 83 %. Annual precipitation amounts circa 2000 mm and varies between 1600–2100 mm (Emck 2007; Bendix et al. 2008; Rollenbeck and Bendix 2011). The region is characterized by slight seasonal variations in precipitation (Fig. 2), allowing a distinction of three hydrological seasons: (i) During January to April humid air masses from NE directions blow over the Amazon lowland with a ~65 % frequency. Southerly winds bring ca. 30 % of precipitation during this season, in which average precipitation ranges between 500–700mm (Rollenbeck and Bendix 2011). (ii) Between May and August wind directions from NE prevail with up to 95 % frequency. Rainfall amounts to as much as 1000 mm. (iii) From September to December average precipitation ranges between 250–420 mm. Furthermore, the highest temperatures of the year are reached during October and November. This short warm and drier period is called 'Veranillo del Niño' and is caused by the increasing influence of wind directions from S (~50 % frequency) and decreasing wind from NE (~45 % frequency), leading to a reduced cloud cover and to more drier days with high irradiation (Bendix et al. 2008; Richter et al. 2009; Rollenbeck and Bendix 2011).

The study species *Cedrela montana* (Moritz ex Turcz) is a rather shade tolerant and deciduous tropical broad-leaved tree species, commonly growing in altitudes between 1700–3000 m a.s.l. in Ecuador, Peru, Venezuela, and Colombia (Smith 1960; RNJB 2008). *C. montana* (Meliaceae) belongs to the mid-successional group of trees, reaches up to 30 m in height and produces a very hard and durable wood (Nieto and Rodriguez 2003; Bräuning et al. 2009; Günter et al. 2009; Kuptz et al. 2010).

3 Sample collection and preparation, cross-dating, cellulose extraction and isotope analysis

Wood samples of *C. montana* were collected as increment cores (5 mm diameter) at the RBSF (Fig. 1) at an elevation of ca. 2000 m a.s.l. A first version of the Cedrela ring width chronology (Bräuning et al. 2009) was extended and updated (unpublished) and now covers the time period 1840–2011. Ring width measurements were carried out using a LINTAB 5 measurement device (Rinntech, Germany) with a precision of 0.01 mm.

Tree cores for oxygen isotope analysis were selected with the following criteria: (i) occurrence of no or only few missing or false rings, (ii) annual rings with straight borders to enable precise separation of annual rings with a razor blade under a binocular microscope and (iii) the ring-width curves of the sampled trees show high correlations to the master chronology, ensuring correct dating of each individual ring. Hence, the selected trees give a good representation of the total sample population. In total, 15 trees, aged up to 120 years, were selected.

To avoid a possible influence of wood chemicals on the oxygen isotope signal we extracted cellulose from the whole tree rings following the chemical treatment described by Wieloch et al. (2011). Afterwards, we homogenized the cellulose with an ultrasonic unit and ca. 300 µg of the freeze-dried material was loaded into silver capsules (Laumer et al. 2009). The tree-ring cellulose was pyrolized in an high temperature oven (Hekatech, Germany) and subsequently transferred to an IRMS (Isotope-ratio mass spectrometer, Delta V Advantage, Thermo Scientific) to detect the $^{18}O/^{16}O$ ratio. The $\delta^{18}O$ values are expressed relative to the VSMOW (Vienna Standard Mean Ocean Water) standard and have an analytic precision of 0.05 ‰ (IAEA 601) and 0.14 ‰ (IAEA 602) and 0.1 ‰ for the cellulose standard (Aldrich). The oxygen isotope values are presented in the δ notification as per mil (‰) and were calculated as $\delta^{18}O_{PNP} = (R_{sample}/R_{standard} -1)$.

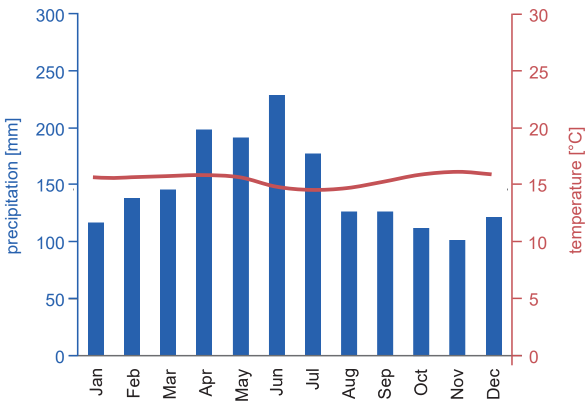

Fig. 2: Mean monthly precipitation (mm) and temperature at the RBSF weather station (2000 m a.s.l., 1998–2011)

4 Datasets and data analysis

Since the local climate data available were too short for statistical calibration of the tree-ring data, we used monthly climate data from Climate Research Unit (CRU) time-series (TS) Version 3.21 (Harris et al. 2014) from the region 3.75°S, 79.25°W (Cordillera Real). Monthly values of the El Niño-Southern Oscillation precipitation Index (ENSO prec., 1979–2009), sea surface temperatures (SSTs) from the El Niño 3.4 (5°S–5°N, 170°–120°W) and 4 (5°S-5°N, 160°E-150°W) regions (1870–2011), and the 3-month running mean of the Oceanic Nino Index (ONI) are from the National Oceanic and Atmospheric Administration (NOAA[1]; Hörling et al. 2001; Rayner et al. 2003). The ONI is an indicator for El Niño events and reflects Pacific Ocean conditions at the equator, where positive/negative values indicate warm/cold temperatures, respectively. Isotope values in precipitation $\delta^{18}O_{prec}$ from Izobamba (0.37°S, 78.55°W) were taken from the Global Network of Isotopes in Precipitation (IAEA/WMO 2015) and were downloaded from Water Isotope System for Data Analysis, Visualization and Electronic Retrieval (WISER). Oxygen isotope data from Peruvian glacier ice cores of Huascarán and Quelccaya were taken from Paleoclimatology Datasets from Thompson et al. (1995, 2013, downloaded via NOAA[2]).

We calculated all Pearson correlation coefficients with IBM SPSS Statistics 22. Because of the lack of normal distribution in the interval-scaled data we also calculated Spearman rank correlation coefficients. However, since all results for Spearman´s correlations were confirmed by Pearson correlations, we do not show Spearman's rank correlations in the following results. Linear regressions between $\delta^{18}O_{prec}$ and $\delta^{18}O_{PNP}$ were carried out with Origin 9.1G. To minimize errors, only years without lacking monthly values in the $\delta^{18}O_{prec}$ were considered. For calculating annual means of $\delta^{18}O_{prec}$ for years missing less than 33% of values, we filled the gaps by averaging the monthly values before and after the missing month (Brienen et al. 2012).

Raw ring width curves were transferred into dimensionless tree-ring index series to remove age-related growth trends. The transformation of raw ring width curves into detrended (spline with 50-year bandwidth to preserve multi-decadal variability in the resulting index curves) dimensionless tree-ring index series and the expressed population signal (EPS) was computed with R package 'dplR' (Bunn 2008). Detrending followed by the "classic nonlinear model of biological growth" described by Bunn and Korpela (2014, 6). As indicator for inter-series correlation between individual tree-ring $\delta^{18}O$ series included in the final chronology, and for chronology reliability, the mean correlation between all isotope series (Rbar) and the expressed population signal (EPS), which is a measure of chronology reliability (Wigley et al. 1984), were computed for running 20-year windows.

5 Results

5.1 Characteristics of the stable isotope chronology

The oldest *C. montana* tree displayed rings as far back as 1885; however, a replication of at least three individuals in the final $\delta^{18}O_{PNP}$ chronology was reached from 1905. The arithmetic mean of the $\delta^{18}O_{PNP}$ chronology for the period 1905–2011(tree individuals) is 26.03 ‰; with values for individual years ranging from 23.8 ‰ to 27.9 ‰ (Fig. 3). The long-term $\delta^{18}O_{PNP}$ trend showed a very weak increase of 0.25 ‰ over the whole study period. Our tree-ring oxygen isotope chronology showed significant inter-series correlations between the single tree isotope series and a robust chronology signal indicated by Rbar statistics (0.18–0.63 from 1938–2011) and EPS (0.85–0.92 from 1938–2011, Fig. 3). Due to low sample replication, values of Rbar and EPS of the chronology are rather low before 1938; hence the chronology prior to 1938 would be improved by finding more old trees. We also tested the individual $\delta^{18}O$ tree-ring series chronology for trends related to tree age (Esper et al. 2010), but no trend related to tree aging was found, making us confident that detected variations of the stable isotope chronology are related to envi-

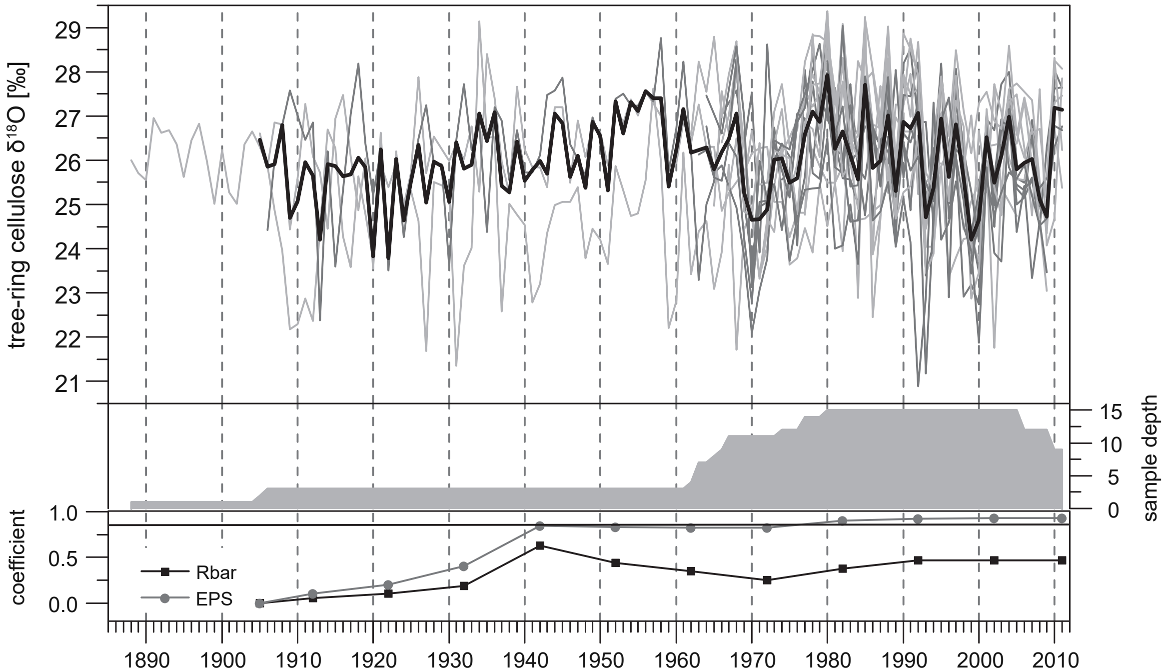

Fig. 3: Tree-ring $\delta^{18}O$ (‰) data from single trees (gray lines) and composite chronology (black line) from 15 trees ($\delta^{18}O_{PNP}$) with sample size, running expressed population signal (EPS) and inter-series correlation (Rbar) calculated for overlapping 20-year intervals

ronmental changes. Therefore, the final tree-ring isotope chronology can be considered to provide robust estimates of local as well as regional environmental changes since 1938.

5.2 Correlations between tree-ring isotopes and climate parameters

We found no significant correlation between the variation in tree-ring $\delta^{18}O_{PNP}$ and annual or seasonal mean of precipitation (r=-0.13), relative humidity (r=-0.29), temperature (r=-0.38), or irradiation (r=-0.2) related to the local climate station data for the period 1998–2011 (detailed results not shown). However, when using CRU TS 3.21 (region 3.75°S, 79.25°W) gridded climate data, the amount of precipitation, cloud cover and wet day frequency are significantly related to $\delta^{18}O_{PNP}$ (Tab. 1).

The months of the main growth period of *C. montana* (January to April) showed the strongest negative correlations. All correlation coefficients increased when the recent time period (1960–2011) was used as compared to the whole century time period (1901–2011): e. g. January to April wet day frequency from r=-0.28 to r=-0.42 (both p<0.01). For cloud cover, data showed for the long period (1901–2011) a significant January to April r=-0.26 (p<0.01) correlation. We also tested for the time period 1901–1959 but no significant correlations between $\delta^{18}O_{PNP}$ and climate parameters were found. After a peak around 1980, the $\delta^{18}O_{PNP}$ values decreased while cloud cover simultaneously increased (Fig. 5) until the strong La Niña event 1999–2000. Cloudiness dropped until 2005 and slightly increased again, showing opposite trends to the $\delta^{18}O_{PNP}$ chronology.

5.3 Teleconnection to other stable isotope records and ENSO

Tree-ring width and $\delta^{18}O_{PNP}$ chronologies of the studied trees were slightly negatively correlated (r=-0.17; p<0.06; n=124), indicating different climatic forces on the two wood parameters. Since tree roots take up soil water without fractionation of soil water $\delta^{18}O$, McCarroll and Loader (2004) nominate precipitation $\delta^{18}O$ as a dominant environmental signal in tree-ring $\delta^{18}O$. The location of our study trees on a steep slope with a good drainage and hence without influence of stagnant ground water, gave us reason to hypothesize that tree-rings reflect variations in precipitation $\delta^{18}O$. To test this, we correlated monthly and annual data of the $\delta^{18}O_{PNP}$ with $\delta^{18}O_{prec}$ from Izobamba (1973–2008, not continuous, ca. 29 % data missing; Tab. 2).

Tab. 1: Pearson correlation coefficients between $\delta^{18}O_{PNP}$ and CRU TS 3.21 data (region 3.75°S, 79.25° W) for wet day frequency, cloud cover, and precipitation

	wet day frequency (days)		cloud cover (%)	precipitation (mm)	
	1901–2011	1960–2011	1901–2011	1901–2011	1960–2011
previous September	-0.16	-0.25	-0.19*	-0.14	-0.11
previous November	-0.19*	-0.35*	-0.10	-0.17	-0.29*
previous December	-0.18	-0.23	-0.08	-0.14	-0.15
previous annual mean	-0.23*	**-0.41****	-0.11	-0.15	-0.23
January	**-0.27****	**-0.37****	-0.22*	-0.19	-0.21
February	**-0.31****	**-0.42****	-0.17	**-0.26****	**-0.42****
March	**-0.26****	-0.35*	-0.22*	-0.20*	-0.35*
April	0.08	-0.04	-0.21*	0.10	0.01
May	-0.14	-0.09	-0.22*	-0.02	0.03
June	-0.06	-0.16	-0.15	-0.09	-0.29*
September	-0.11	-0.09	-0.12	-0.19*	-0.18
October	-0.05	0.00	-0.20*	-0.03	0.09
current annual mean	**-0.25****	-0.33*	-0.24*	-0.20*	-0.31*
January to April	**-0.28****	**-0.42****	**-0.26****	-0.17	-0.32*
May to August	-0.13	-0.16	-0.19*	-0.07	-0.19

$p<0.01$, $^*p<0.05$

Tab. 2: Pearson correlation coefficients between Izobamba $\delta^{18}O_{prec}$ and $\delta^{18}O_{PNP}$ (1973–2008)

Jan	Feb	Mar	Apr	May	Jun	Jul	Aug	Sep	Oct	Nov	Dec	Annual Mean
0.44	0.38	0.00	0.21	0.33	0.06	0.01	-0.22	0.18	0.28	**0.70****	0.30	**0.57****

$^{**}p<0.01$

We found a significant positive relationship for precipitation of the annual mean and for the drier season month November ('Veranillo del Niño'; Richter et al. 2009; Tab. 2; Fig. 4). During the less humid period the major influence of $\delta^{18}O_{prec}$ is verifiable, while in the other months no significant correlations occur. To verify the detected relationship, we tested the correlations between $\delta^{18}O_{prec}$ from Izobamba and ENSO parameters (Tab. 3).

We compared our results with other available hydroclimate archives located around the Amazon Basin, including $\delta^{18}O$ from high-elevation ice cores from the central Andean glaciers Quelccaya (13.56°S, 70.50°W; 5670 m a.s.l.) and Huascarán (9.06°S, 77.36°W; 6048 m a.s.l.) (Thompson et al. 1995, 2013). We found positive correlations between $\delta^{18}O_{PNP}$ and the Huascarán ice cap, which is located closer to our study site but in higher elevation than Quelccaya. Both glaciers receive

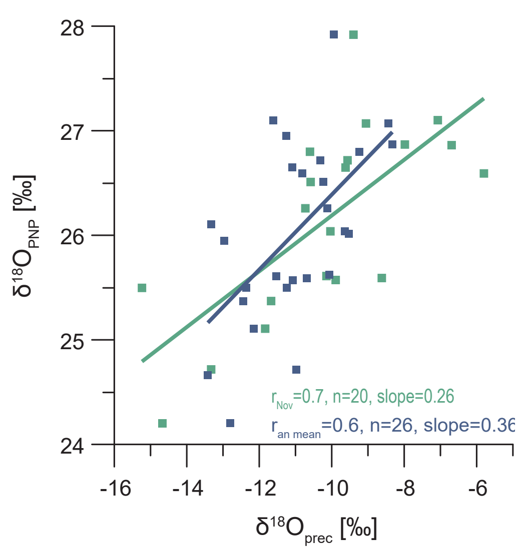

Fig. 4: Relationship ($p<0.001$) between $\delta^{18}O_{PNP}$(‰) and $\delta^{18}O_{prec}$(‰) in Izobamba precipitation during November and for the entire year

Tab. 3: Pearson correlation coefficients between Izobamba $\delta^{18}O_{prec}$ and ENSO (1979–2008)

	ENSO prec. Index	El Niño 3.4	El Niño 4
$\delta^{18}O_{prec}$	**-0.49***	0.45	**0.49***

***p<0.05**

moisture from the Amazon basin (Thompson et al. 2013) and are therefore impacted by the same dominant wind direction as our study site in southern Ecuador. Correlations are stronger for the period after 1960 than for the whole period 1885–2009 covered by our ^{18}O-chronology (Tab. 4).

The main factors of inter-annual variation of precipitation in the study area are the humid air masses from the Amazon basin transported by the tropical easterlies (Rollenbeck and Bendix 2011). In turn, the moisture conditions in the Amazon basin are influenced by ENSO (Brienen et al. 2012). For the period after 1960, we found a positive correlation between $\delta^{18}O_{PNP}$ and SSTs in the El Niño 3.4 and 4 regions in the equatorial Pacific (Tab. 5). Weak and non-significant correlations occur for the time period 1885–2011 for both El Niño 3.4 and 4 regions. The strongest impact on $\delta^{18}O_{PNP}$ occurs during austral summer from previous October to February, when correlations ranged between 0.28 ($p<0.05$, February El Niño 3.4, 1960–2011) to 0.48 ($p<0.01$, February El Niño 4, 1975–2011) (Tab. 5). The ONI (1950–2011) also showed a strong positive correlation during previous December to recent February. Contrary, the ENSO precipitation index showed strong negative correlations with the oxygen isotope chronology for the time period 1979–2011. Moreover, strong La Niña events like 1973–1976, 1999–2000, and 2010–2011 are traceable in the $\delta^{18}O_{PNP}$ chronology by lower $\delta^{18}O$ values related to the higher amounts of precipitation in the Andean mountains (Fig. 5).

Tab. 4: Pearson correlation coefficients between $\delta^{18}O_{PNP}$ and oxygen isotopes from ice cores of Andean glaciers in Peru

	Quelccaya		Huascarán 1		Huascarán 2		Mean Huascarán	
	1885–2009	1960–2009	1894–1993	1960–1993	1894–1993	1960–1993	1894–1993	1960–1993
$\delta^{18}O_{PNP}$	0.19*	0.40*	0.16	**0.49****	0.21*	**0.51****	0.20*	**0.53****

****p<0.01**, *p<0.05

Tab. 5: Pearson correlation coefficients between $\delta^{18}O_{PNP}$ and sea surface temperatures in El Niño 3.4 and 4 regions, ENSO precipitation Index and Oceanic Niño Index (ONI)

	El Niño 3.4[1]			El Niño 4[1]			ENSO prec.[2]	ONI[3]
	1885–2011	1960–2011	1975–2011	1885–2011	1960–2011	1975–2011	1979–2011	1950–2011
previous September								
previous October			0.32*		0.28*	0.33*		
previous November			0.34*		0.28*	0.36*		
previous December		0.31*	0.38*		0.34*	0.41*		0.26*
January		0.31*	0.38*		0.35*	**0.45****	-0.39*	0.26*
February		0.28*	0.37*		**0.35****	**0.48****	-0.34*	0.26*
March						**0.45****	**-0.49****	
April						0.37*	-0.40*	
January to April	0.11	0.28*	0.34*	0.17	0.34*	**0.46****	**-0.47****	

****p<0.01**, *p<0.05

[1] Sea Surface Temperature

[2] El Niño – Southern Oscillation precipitation Index

[3] Oceanic Nino Index

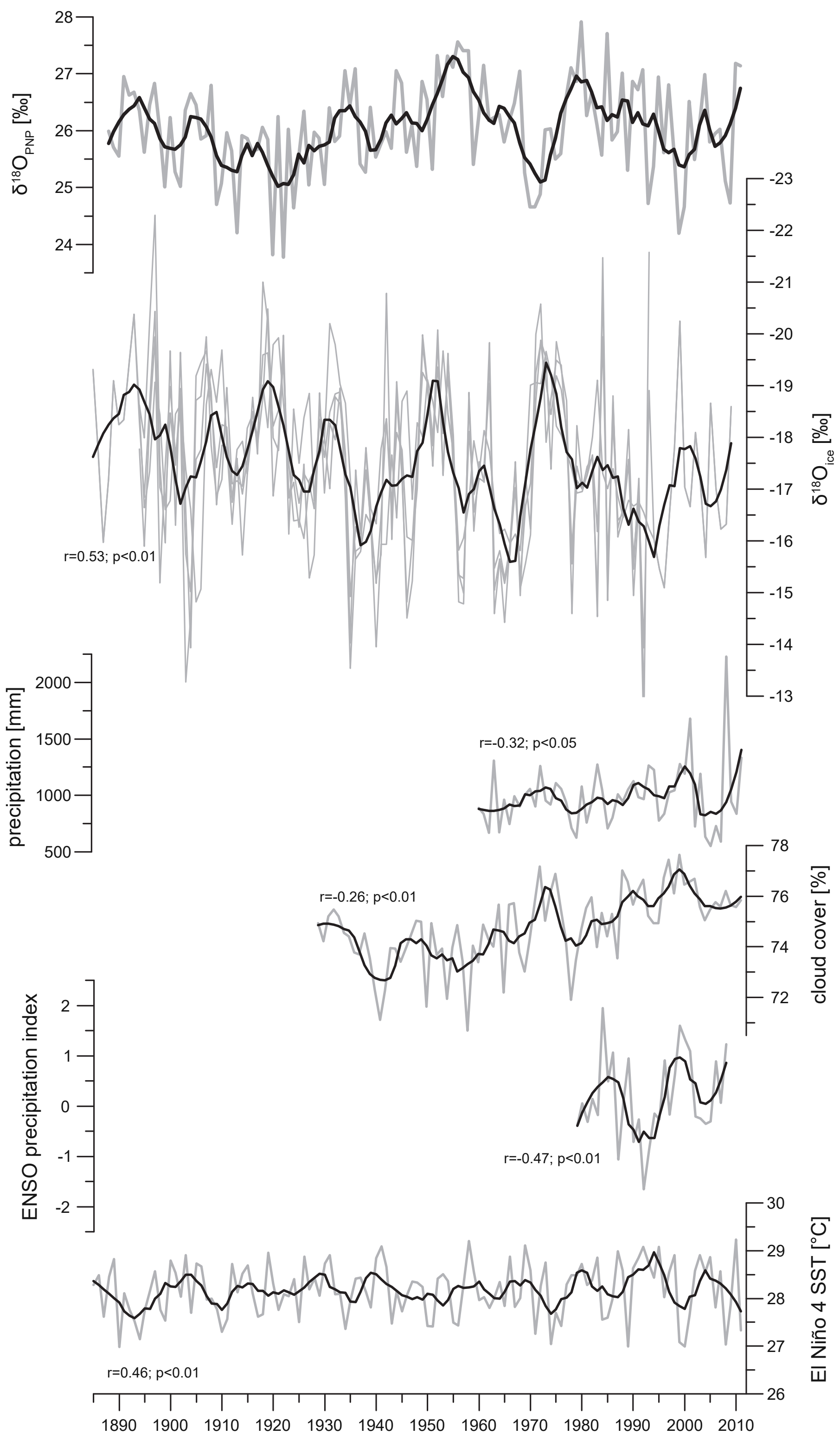

Fig. 5: From top to down: time series of the $\delta^{18}O_{PNP}$ chronology, data from Quelccaya and Huascarán1 and 2 as well as the mean of $\delta^{18}O_{ice}$ values, precipitation and cloud cover from CRU TS 3.21 and January to April mean of ENSO precipitation Index as well as El Niño 4 SST. Bold lines show smoothed data series with a 10-year FFT filter

6 Discussion

The $\delta^{18}O$ values of the 15 studied *C. montana* trees significantly correlated between each other and showed a strong common signal (Fig. 3). The highest EPS occurred after 1930, with minimum values round 1960. This could be a result of dating errors of some individual rings during the juvenile growth phase and hence a misdating of measured oxygen isotopes. Compared to other studies, the strength of our common $\delta^{18}O$ signal (mean EPS=0.86 1938–2011) is slightly higher than reported for trees from Cameroon (mean EPS=0.74 1930–2010; van der Sleen et al. 2015) and Laos (mean EPS=0.8 1951–2001; Xu et al. 2011), but marginally lower than for trees from Bolivia (mean EPS=0.93 1900–2001; Brienen et al. 2012) or Indonesia (mean EPS=0.9 1900–2007; Schollean et al. 2013). A possible explanation is the lower climate variability at our study site, which has continuously high precipitation and a relatively low interannual variability of $\delta^{18}O_{PNP}$ in comparison to other studies (Poussart and Schrag 2005).

The long-term $\delta^{18}O_{PNP}$ increasing trend of 0.25 ‰ from 1885 to 2011 (Fig. 5) is weaker than trends reported from Bolivia (Brienen et al. 2012), Cameroon (van der Sleen et al. 2015), Thailand (Poussart and Schrag 2005), Laos (Xu et al. 2011), and Vietnam (Sano et al. 2012). In South East Asia, the stronger increase is in line with a weakening of the Asian Monsoon (Poussart and Schrag 2005; Xu et al. 2011). In Africa, the great Sahel drought from 1970 to 1990 influenced the long-term trend in tree-ring $\delta^{18}O$ (van der Sleen et al. 2015). For South America, a positive trend of $\delta^{18}O$ in climate proxies is reported by Thompson et al. (2013) for $\delta^{18}O$ in ice cores and for trees in the Amazon basin (Brienen et al. 2012). This may point to an overall increasing temperature (3K relative to the average of 1980–1999) trend together with a slight increase in rainfall (+ 8 %) and cloud cover (+4 %) over the Andes in southern Ecuador (Meehl et al. 2007; Gloor et al. 2013; Peters et al. 2013).

We did not find any influence of biological tree age on $\delta^{18}O_{PNP}$, as it was reported in other studies (e.g. Kahmen et al. 2011; Barbour 2007; Esper et al. 2010). A possible explanation may be the low variability of measured relative humidity and temperature, and the resulting small vapor pressure deficit experienced by trees at the study site. Age-effects strongly depend on site conditions and species (van der Sleen et al. 2015). No age-related long-term trend in $^{18}O_{PNP}$ was found (Fig. 3), which is consistent with numerous other studies (e.g. van der Sleen et al. 2015; Brienen et al. 2012; Zhu et al. 2012; Sano et al. 2012; Xu et al. 2013b).

To quantify the effects of leaf transpiration on the $\delta^{18}O$ variation in tree-rings, we tested the correlations of local amounts of precipitation, irradiation, temperature, relative humidity, and vapor pressure deficit with tree-ring oxygen isotopes (1998–2011). The detected relationships were not statistically significant; hence we conclude that the influence of meteoric precipitation composition is higher for our studied trees than the local climate. Van der Sleen et al. (2015) also did not find strong correlations between local climate signals (e.g. precipitation, temperature) and tree-ring $\delta^{18}O$ in *Entandrophragma utile* in Cameroon. These trends indicate a strong influence of global circulation and regional climate on $\delta^{18}O$ variation in tropical tree-rings.

The significant correlations with the gridded CRU TS 3.21 data suggested that under the local per humid conditions, trees store the regional ^{18}O precipitation signal in their cellulose (Tab. 1). The trees rather reflect the water-vapor-transport over the Andes than the stationary precipitation amount at the site, as found by other studies (van der Sleen et al. 2015; Brienen et al. 2012; Poussart and Schrag 2005; Xu et al. 2011, 2013a, b; Sano et al. 2012). Low correlation coefficients with wet day frequency and precipitation may partly also be a result of poor quality and spatial resolution of meteorological data prior to 1960. The findings, that tree-ring oxygen isotopes are controlled by humidity (correlations to CRU TS 3.21 precipitation) suggested that the amount of precipitation during January to April and the entire year influenced $\delta^{18}O_{PNP}$ very strongly. Periods of less rainfall and higher irradiation go hand in hand with higher $\delta^{18}O_{PNP}$ values, for instance during 1950s and the 1980s. The decreasing trend of $\delta^{18}O_{PNP}$ since 1980 is in line with an increasing precipitation rate and cloud cover in the region. However, the declining trend reversed in 2000, values reached a maximum 2005 and thereafter, moisture conditions within the atmosphere increased again.

Goller et al. (2005) investigated $\delta^{18}O$ in precipitation within the RBSF from September 2000 to August 2001. The annual RBSF $\delta^{18}O_{prec}$ values range between -8 ‰ and -16 ‰. During January to April, $\delta^{18}O_{prec}$ values decrease from -8 ‰ to -16 ‰, then increase continually to -8 ‰ (August, with main wind direction NE from the Amazon Basin) and thereafter decrease slightly to -10 ‰/-9 ‰ in November/ December. This observed annual cycle is also shown by the annual variation of the Izobamba $\delta^{18}O_{prec}$ values (Fig. 4, Tab. 3). In fact, the meteoric $\delta^{18}O$ values are related to different air-masses brought into the study area by a seasonal change of dominant wind directions (Rollenbeck and Bendix 2011). Inflows between September and April are balanced between southerly and northerly directions, whereas from May to August, northerly wind directions dominate. Westerly and easterly winds deliver equal portions of precipitation (Rollenbeck and Bendix 2011). Hence, it appears that $\delta^{18}O$ in precipitation from westerly winds (Pacific) more reflected in tree ring $\delta^{18}O_{prec}$ ratios, especially in the drier season.

The $\delta^{18}O_{ice}$ variations from the Andean glaciers demonstrate the dominant inflow of Amazon air masses at the 500 and 850 hPa level throughout the year. The ice core oxygen isotope records show strong year-to-year fluctuations in comparison to $\delta^{18}O_{PNP}$ (Fig. 5, Tab. 4). This is caused by the ascending air masses on the Andean mountain chain and the following $\delta^{18}O$ rainout process (Thompson et al. 2000; Vuille et al. 2003). The observed high correlations between $\delta^{18}O_{PNP}$ and $\delta^{18}O_{ice}$ demonstrate the intense influence of Amazon moisture on the trees within the lower montane rainforest. Also decadal variations of $\delta^{18}O_{ice}$ from Quelccaya records are traceable within the tree ring oxygen isotopes (Thompson et al. 2013).

Moreover, we found stationary correlations to El Niño 4 SST, e.g. for 1955–1985 (Tab. 5), which coincided with the shift of the Pacific Ocean climate regime (Mantua and Hare 2002). The $\delta^{18}O_{PNP}$ is also influenced by the "Pacific moisture", as discussed in the comparison with meteoric precipitation $\delta^{18}O$ from Izobamba. The detected effect of rainfall amount and composition on the isotopic composition is in accordance with the investigations of Sturm et al. (2007) and Vuille et al. (2005). Vuille et al. (2005) pointed out that both, tropical Pacific and tropical Atlantic atmospheric circulations affect precipitation and $\delta^{18}O$ variability over the Andes. The influence from the lower to the upper troposphere increases. Spatial and temporal variations of $\delta^{18}O_{prec}$ strongly differ between seasons. During austral summer, isotope variations in the Andes are controlled by air-mass-transport from the Amazon basin (Sturm et al. 2007). Vimeux et al. (2009) reported enriched $\delta^{18}O$ values during El Niño events and depleted $\delta^{18}O$ values during La Niñas in ice core records of the Andean glaciers. This is reflected in the tree-ring oxygen isotope values, however, with varying strength.

Correlations of the $\delta^{18}O_{PNP}$ in the Cordillera Real and the ENSO precipitation Index as well as the SSTs of El Niño 3.4 and 4 regions and the ONI indicate (Tab. 5) a large-scale atmospheric circulation control of the regional climatic conditions. In different tropical regions around the globe, an ENSO effect on oxygen isotope variations in tree-rings was found (Poussart and Schrag 2005; Anchukaitis et al. 2008; Xu et al. 2011, 2013a, b; Brienen et al. 2012; Sano et al. 2012; Zhu et al. 2012). The ENSO influence on our isotope records was especially strong in the 1960s, whereas during the first half of the 20th century the influence was weak or not significant. A reason could be the lower variance of ENSO in the CRU TS data, because data before 1961 are reconstructed from the 1961–1990 'normal values'. In addition, the positive relationship between $\delta^{18}O_{PNP}$ and Pacific SSTs (Tab. 5) points to an effect on the austral summer season climate in RBSF by the Pacific westerlies. However, our results indicated that tree-ring $\delta^{18}O_{PNP}$ can be used to reconstruct single ENSO (SSTs) events during the season January to April.

While El Niño events did not stand out in the isotope chronologies, La Niña events were represented by pronounced $\delta^{18}O_{PNP}$ minima, which is in line with studies in Laos (Xu et al. 2011, 2013b) and Cambodia (Zhu et al. 2012). The strong La Niña event 1973–1976 represents the minimum value in the whole chronology (Fig. 5). Different authors described this event as a shift in the climate regime of the Pacific Ocean (Deser et al. 2004; Zhu et al. 2012) from a "warm" Pacific Decadal Oscillation (PDO) starting 1976/77 and lasting until the strong La Niña 1999/2000 (Mantua and Hare 2002). The "warm" PDO was related to a wetter, warmer, and cloudier period over the Andes.

7 Conclusions and perspectives

In this paper, we presented a new tree-ring oxygen isotope record composed of fifteen individual *C. montana* trees from the Cordillera Real in the Andes. The $\delta^{18}O_{PNP}$ record correlated to precipitation and moisture conditions during the last century at regional and continental scales. This connection is established by the following proxies: SSTs of the tropical Pacific, ENSO precipitation Index and PDO. Considering that *C. montana* forms annuals rings, has both the potential for long life and a wide geographic distribution, makes it a useful species to reconstruct climate in the Andes. The isotopic signal suggested that rather than local climatic effects, water-vapor transport from the Amazon basin into the Andes on the one hand, and the Pacific circulation on the other hand, control stable isotope variations in mountain rainforest trees. The oxygen isotope ratios in tree-rings documented the averaged isotopic composition of the meteoric rainfall for the year of growth and showed significant correlations with Andean glacier ice core records. One of the most important results is the large-scale control of $\delta^{18}O_{PNP}$ by ENSO, with an increasing influence during the last decades, suggesting changing atmospheric circulation processes over the Andes. The last "warm" PDO period is detectable within the $\delta^{18}O_{PNP}$ chronology. However, the oxygen isotope trend increased slightly (0.25 ‰) during the studied period from 1885–2011. A higher temporal resolution of intra-annual $\delta^{18}O$ variability in tree-rings (e.g. Poussart and Schrag 2005; Anchukaitis et al. 2008) is a possible tool to gain better insight into changing seasonal regional circulation patterns.

Thus, we encourage the establishment of an ENSO-sensitive tree-ring network within the Andes to improve our understanding of spatial and temporal teleconnections of ENSO variability over equatorial South America.

Acknowledgements

We thank Susanne Spannl, Wolfgang Pfautsch, Roswitha Höfner-Stich, and Dr. Christoph Mayr for technical assistance and helpful comments. This study was supported by the German Research Foundation (DFG) by funding the projects BR 1895/14-1/2 (FOR 816) and BR 1895/23-1 (PAK 823). Furthermore, special thanks go to the anonymous reviewer who helped to improve the manuscript considerably.

References

Anchukaitis, K. J.; Evans, M. N.; Wheelwright, N. T. and Schrag, D. P. (2008): Stable isotope chronology and climate signal calibration in neotropical montane cloud forest trees. In: Journal of Geophysical Research 113, G03030. DOI: 10.1029/2007JG000613

Ballantyne, A. P.; Baker, P. A.; Chambers, J. Q.; Villalba, R. and Argollo, J. (2011): Regional differences in South American monsoon precipitation inferred from the growth and isotiopic composition of tropical trees. In: Earth Interactions 15, 1–35. DOI: 10.1175/2010EI277.1

Balselv, H. and Øllgaard, B. (2002): Mapa de vegetaciónes del sur de Ecuador. Botánica height Austroecuatoriana. Quito.

Barbour; M. M. (2007): Stable oxygen isotope composition of plant tissue: a review. In: Functional Plant Biology 34, 83–94. DOI: 10.1071/fp06228

Bendix, J.; Rollenbeck, R.; Fabian, P.; Emck, P.; Richter, M. and Beck, E. (2008): Climatic variability. In: Beck, E.; Bendix, J.; Kottke, I.; Makeschin, F. and R. Mosandl (eds.): Gradients in a tropical mountain ecosystem of Ecuador. Berlin, Heidelberg, 281–290. DOI: 10.1007/978-3-540-73526-7_27

Bradley, R. S.; Vuille, M.; Hardy, D. and Thompson, L. G. (2003): Low latitude ice cores record Pacific sea surface temperatures. In: Geophysical Research Letters, 30, 1174. DOI: 10.1029/2002GL016546

Bräuning, A.; Volland-Voigt, F.; Burchardt, I.; Ganzhi, O.; Nauss, T. and Peters, T. (2009): Climatic control of radial growth of *Cedrela montana* in a humid mountain rain forest in southern Ecuador. In: Erdkunde 63, 337–345. DOI: 10.3112/erdkunde.2009.04.04

Brienen, R. J. W.; Helle, G.; Pons, T. L.; Guyot, J.-L. and Gloor, M. (2012): Oxygen isotopes in tree rings are a good proxy for Amazon precipitation and El Niño-Southern Oscillation variability. In: PNAS 109, 16957–16962. DOI: 10.1073/pnas.1205977109

Bunn, A. (2008): A dendrochronology program library in R. In: Dendrochronologia 26, 115–124. DOI: 10.1016/j.dendro.2008.01.002

Bunn, A. and Korpela, M. (2014): An introduction to dplR. Dendrochronology Program Library in R. http://cran.r-project.org/web/packages/dplR/dplR.pdf (05.09.2014)

Dansgaard, W. (1964): Stable isotopes in precipitation. In: Tellus 16, 436–468. DOI: 10.1111/j.2153-3490.1964.tb00181.x

Deser, C.; Phillips, A. S. and Hurrell, J. W. (2004): Pacific interdecadal climate variability: linkages between the tropics and the North Pacific during boreal winter since 1900. In: Journal of Climate 17, 3109–3124. DOI: 10.1175/1520-0442(2004)017<3109:PICVLB>2.0.CO;2

Emck, P. (2007): A climatology of South Ecuador. PhD thesis. Erlangen.

Esper, J.; Frank, D. C.; Battipaglia, G.; Büntgen, U.; Holert, C.; Treydte, K.; Siegwolf, R. and Saurer, M. (2010): Low-frequency noise in $\delta^{13}C$ and $\delta^{18}O$ tree ring data: a case study of *Pinus uncinata* in the Spanish Pyrenees. In: Global Biogeochemical Cycles 24, GB4018. DOI: 10.1029/2010GB003772

Gessler, A.; Ferrio, J. P.; Hommel, R.; Treydte, K.; Werner, R. A. and Monson, R. K. (2014): Stable isotopes in tree rings: towards a mechanistic understanding of isotope fractionation and mixing processes from the leaves to the wood. In: Tree Physiology 34, 125–134. DOI: 10.1093/treephys/tpu040

Gloor, M.; Brienen, R. J. W.; Galbraith, D.; Feldpausch, T. R.; Schöngart, J.; Guyot, J.-L.; Espinoza, J. C.; Lloyd; J. and Phillips, O. L. (2013): Intensification of the Amazon hydrological cycle over the last two decades. In: Geophysical Research Letters 40, 1729–1733. DOI: 10.1002/grl.50377

Goller, R.; Wilke, W.; Leng, M. J.; Tobschall, H. J.; Wagner, K.; Valarezo, C. and Zech, W. (2005): Tracing water paths through small catchments under tropical montane rain forest in South Ecuador by an oxygen isotope approach. In: Journal of Hydrology 308, 67–80. DOI: 10.1016/j.jhydrol.2004.10.022

Günter, S.; Gonzalez, P.; Álvarez, G.; Aguirre, N.; Palomeque, X.; Haubrich, F. and Weber, M. (2009): Determinants for successful reforestation of abandoned pastures in the Andes: soil conditions and vegetation cover. In: Forest Ecology and Management 258, 81–91. DOI: 10.1016/j.foreco.2009.03.042

Harris, I.; Jones, P. D.; Osborn, T. J. and Lister, D. H. (2014): Updated high-resolution grids of monthly climatic observations – the CRU TS3.10 Dataset. In: International Journal of Climatology 34, 623–642. DOI: 10.1002/joc.3711

Hoffmann, G.; Ramirez, E.; Taupin, J. D.; Francou, B.; Ribstein, P.; Delmas, R.; Dürr, H.; Gallaire, R.; Simões, J.; Schotterer, U.; Stievenard, M. and Werner, M. (2003): Coherent isotope history of Andean ice cores over the last century. In: Geophysical Research Letters, 30, 1179. DOI: 10.1029/2002GL014870

Homeier, J. (2004): Baumdiversität. Waldstruktur und Wachstumsdynamik zweier tropischer Bergregenwälder in Ecuador und Costa Rica. PhD thesis. Bielefeld.

Hörling, M. P.; Kumar, A. and Xu, T. (2001): Robustness of the nonlinear climate response to ENSO's extreme phases. In: Journal of Climate 14, 1277–1293. DOI: 1520-0442(2001)014<1277:ROTNCR>2.0.CO;2

IAEA/WMO (2015): Global network of isotopes in precipitation. The GNIP Database. http://www-naweb.iaea.org/napc/ih/IHS_resources_gnip.html (Date: 23.02.2015)

Kahmen, A.; Sachse, D.; Arndt, S. K.; Tu, K. P.; Farrington, H.; Vitousek, P. M. and Dawson, T. E. (2011): Cellulose $\delta^{18}O$ is an index of leaf-to-air vapor pressure difference (VPD) in tropical plants. In: PNAS 108, 1981–1986. DOI: 10.1073/pnas.1018906108

Kuptz, D.; Grams, T. E. E. and Günter, S. (2010): Light acclimation of four native tree species in felling gaps within a tropical mountain rainforest. In: Trees 24, 117–127. DOI: 10.1007/s00468-009-0385-1

Laumer, W.; Andreau, L.; Helle, G.; Schleser, G.; Wieloch, T. and Wissel, H. (2009): A novel approach for the homogenization of cellulose to use micro-amounts for stable isotope analyses. In: Rapid Communications Mass Spectrometry 23, 1934–1940. DOI: 10.1002/rcm.4105

Liu, X.; Xu, G, Griessinger, J.; An, W.; Wang, W.; Zeng, X.; Wu, G. and Qin, D. (2014): A shift in cloud cover over the southeastern Tibetan Plateau since 1600: evidence from regional tree-ring $\delta^{18}O$ and its linkages to tropical oceans. In: Quaternary Science Reviews 88, 55–68. DOI: 10.1016/j.quascirev.2014.01.009

Mantua, N. J. and Hare, S. R. (2002): The Pacifical Decadal Oscillation. In: Journal of Oceanography 58, 34–44. DOI: 10.1023/A:1015820616384

McCarroll, D. and Loader, N. J. (2004): Stable isotopes in tree rings. In: Quaternary Science Reviews 23, 771–801. DOI: 10.1016/j.quascirev.2003.06.017

Meehl, G. A.; Stocker, T. F.; Collins, W. D.; Friedlingstein, P.; Gaye, A. T.; Gregory, J. M.; Kitoh, A.; Knutt, R.; Murphy, J. M.; Noda, A.; Raper, S. C. B.; Watterson, I. G.; Weaver, A. J. and Zhao, Z.-C. (2007): Global climate projections. In: Solomon, S.; Qin, D.; Manning, M.; Chen, Z.; Marquis, M.; Avery, K. B.; Tignor, M. and H. L. Miller (eds.): Climate change 2007: the physical science basis. Contribution of Working Group I to the Fourth Assessment Report of the Intergovernmental Panel on Climate Change. Cambridge, New York, 748–844.

Nieto, V. M. and Rodriguez, J. (2003): *Cedrela montana* Moritz x Turcz. In: Vozzo, J. A. (ed.): Tropical tree seed manual. Washington, 384–385.

NOAA[1] (National Oceanic and Atmospheric Administration) http://www.esrl.noaa.gov/psd/data/climateindices/list/index.html (Date: 23.02.2015)

NOAA[2] (National Oceanic and Atmospheric Administration) http://www.ncdc.noaa.gov/data-access/paleoclimatology-data/datasets/ice-core (Date: 03.03.2015)

Peters, T.; Drobnik, T.; Meyer, H.; Rankl, M.; Richter, R.; Rollenbeck, R.; Thies, B. and Bendix, J. (2013): Environmental changes affecting the Andes of Ecuador. In: Bendix, J.; Beck, E.; Bräuning, A.; Makeschin, F.; Mosandl, R.; Scheu, S. and Wilcke, W. (eds.): Ecosystems services, biodiversity and environmental change in a tropical mountain ecosystem of South Ecuador. Berlin, Heidelberg, 19–29. DOI: 10.1007/978-3-642-38137-9_2

Poussart, P. F. and Schrag, D. F. (2005): Seasonally resolved stable isotope chronologies from northern Thailand deciduous trees. In: Earth and Planetary Letters 235, 752–765. DOI: 10.1016/j.epsl.2005.05.012

Rayner, N. A.; Parker, D. E.; Horton, E. B.; Folland, C. K.; Alexander, L. V.; Rowell, D. P.; Kent, E. C. and Kaplan, A. (2003): Global analyses of sea surface temperature, sea ice, and night marine air temperature since the late nineteenth century. In: Journal of Geophysical Research 108 (D14), 4407. DOI: 10.1029/2002JD002670

RNJB (Red Nacional de Jardines Botánicos) (2008): *Cedrela montana* Moritz ex Turcz.

Richter, M.; Diertl, K. H.; Emck, P.; Peters, T. and Beck, E. (2009): Reasons for an outstanding plant diversity in the tropical Andes of southern Ecuador. In: Landscape Online 12, 1–35. DOI: 10.3097/lo.200912

Richter, M.; Beck, E.; Rollenbeck, R. and Bendix, J. (2013): The study area. In: Bendix; J.; Beck, E.; Bräuning, A.; Makeschin, F.; Mosandl, R.; Scheu, S. and Wilcke; W. (eds.): Ecosystem services, biodiversity and environmental change in a tropical mountain ecosystem of South Ecuador. Berlin, Heidelberg, 1–19. DOI: 10.1007/978-3-642-38137-9_1

Rollenbeck, R. and Bendix, J. (2011): Rainfall distribution in the Andes of southern Ecuador derived from blending weather radar data and meteorological field observations. In: Atmospheric Research 99, 277–289. DOI: 10.1016/j.atmosres.2010.10.018

Rozendaal, D. M. A.; Brienen, R. J. W.; Soliz-Gamboa, C. C. and Zuidema, P. A. (2010): Tropical tree rings reveal preferential survival of fast-growing juveniles and increased juvenile growth rates over time. In: New Phytologist 185, 759–769. DOI: 10.1111/j.1469-8137.2009.03109.x

Sano, M.; Xu, C and Nakatsuka, T. (2012): A 300-year Vietnam hydroclimate and ENSO variability record reconstructed from tree-ring $\delta^{18}O$. In: Journal of Geophysical Research 117, D12115. DOI: 10.1029/2012JD017749

Schollean, K.; Heinrich, I.; Neuwirth, B.; Krusic, P. J.; D'Arrigo, R. D.; Karyanto, O. and Helle, G. (2013): Multiple tree-ring chronologies (ring-width, $\delta^{13}C$ and $\delta^{18}O$) reveal dry and rainy season signals of rainfall in Indonesia. In: Quaternary Science Reviews 73, 170–181. DOI: 10.1016/j.quascirev.2013.05.018

Schöngart, J.; Piedade, M. T. F.; Ludwigshausen, S.; Horna, V. and Worbes, M. (2002): Phenology and stem-growth periodicity of tree species in Amazonian floodplain forests. In: Journal of Tropical Ecology 18, 581–597. DOI: 10.1017/s0266467402002389

Smith, C. E. Jr (1960): A revision of Cedrela (Meliaceae). In: Fieldiana Botany 29. Chicago.

Soliz-Gamboa, C. C.; Sandbrink, A. and Zuidema, P. A. (2012): Diameter growth of juvenile trees after gap formation in a Bolivian rain forest: responses are strongly species-specific and size-dependent. In: Biotropica 44, 312–320. DOI: 10.1111/j.1744-7429.2011.00803.x

Stahl, C.; Burban, B.; Bompy, F.; Jolin, Z. B.; Sermage, J. and Bonal, D. (2010): Seasonal variation in atmospheric relative humidity contributes to explaining seasonal variation in trunk circumference of tropical rainforest trees in French Guiana. In: Journal of Tropical Ecology 26, 393–405. DOI: 10.1017/S0266467410000155

Sternberg, L. and DeNiro, M. J. (1983): Isotopic composition of cellulose from C3, C4, and CAM plants growing. In: Science 220, 947–949. DOI: 10.1126/science.220.4600.947

Sternberg, L.; DeNiro, M. J. and Ajie, H. O. (1986): Isotopic relationships between saponifiable lipids and cellulose nitrate prepared from red, brown and green algae. In: Planta 169, 320–324. DOI: 10.1007/BF00392126

Sturm, C.; Hoffmann, G. and Langmann, B. (2007): Simulation of the stable water isotopes in precipitation over South America: comparing regional to global circulation models. In: Journal of Climate 20, 3730–3750. DOI: 10.1175/JCLI4194.1

Thompson, L. G.; Mosley-Thompson, E.; Davis, M. E.; Lin, P.-N.; Henderson, K. A.; Cole-Dai, J.; Bolzan, J. F. and Liu, K.-B. (1995): Late Glacial Stage and Holocene tropical ice core records from Huascarán, Peru. In: Science 269, 46–50. DOI: 10.1126/science.269.5220.46

Thompson, L. G.; Mosley-Thompson, E. and Henderson, K. A. (2000): Ice-core palaeoclimate records in tropical South America since the Last Glacial Maximum. In: Journal of Quaternary Science, 15 (4), 377–394. DOI: 10.1002/1099-1417(200005)15:4<377::AID-JQS542>3.0.CO;2-L

Thompson, L. G.; Mosley-Thompson, E.; Davis, M. E.; Zagorodnov, V. S.; Howat, I. M.; Mikhalenko, V. N. and Lin, P.-N. (2013): Annually resolved ice core records of tropical climate variability over the past ~1800 years. In: Science 340, 945–950. DOI: 10.1126/science.1234210

Treydte, K.; Boda, S.; Graf Pannatier, E.; Fonti, P.; Frank, D.; Ullrich, B.; Sauer, M.; Siegwolf, R.; Battipaglia, G.; Werner, W. and Gessler, A. (2014): Seasonal transfer of oxygen isotopes from precipitation and soil to the tree ring: source water versus needle water enrichment. In: New Phytologist, 1–12. DOI: 10.1111/nph.12741

Van der Sleen, P.; Groenendijk, P. and Zuidema, P. A. (2015): Tree-ring δ18O in African mahogany (Entandrophragma utile) records regional precipitation and can be used for climate reconstructions. In: Global and Planetary Change 127, 58–66. DOI: 10.1016/j.gloplacha.2015.01.014

Villacis, M.; Vimeux, F. and Taupin, J. D. (2008): Analysis of the climate controls on the isotopic composition of precipitation ($\delta^{18}O$) at Nuevo Rocafuerte, 74.5°W, 0.9°S, 250 m, Ecuador. In: Geoscience 340, 1–9. DOI: 10.1016/j.crte.2007.11.003

Vimeux, F.; Ginot, P.; Schwikowski, M.; Vuille, M.; Hoffmann, G.; Thompson, L. G. and Schotterer, U. (2009): Climate variability during the last 1000 years inferred from Andean ice cores: a review of methodology and recent results. In: Palaeogeography, Palaeoclimatology, Palaeoecology 281, 229–241. DOI: 10.1016/j.palaeo.2008.03.054

Volland-Voigt, F.; Bräuning, A.; Ganzhi, O.; Peters, T. and Maza, H. (2011): Radial stem variations on *Tabebuia chrysantha* (Bignoniaceae) in different tropical forest ecosystems of southern Ecuador. In: Trees 25, 39–48. DOI: 10.1007/s00468-010-0461-6

Vuille, M. and Werner, M. (2005): Stable isotopes in precipitation recording South American summer monsoon and ENSO variability: observations and model results. In: Climate Dynamics 25, 401–413. DOI: 10.1007/s00382-005-0049-9

Vuille, M.; Bradley, R. S.; Healy, R.; Werner, M. Hardy, D. R.; Thompson, L. G. and Keimig, F. (2003): Modeling $\delta^{18}O$ in precipitation over the tropical Americans: 2. Simulation of the stable isotope signal in Andean ice cores. In: Journal of Geophysical Research 108, D64175. DOI: 10.1002/2001JD002039

WISER (Water Isotope System for Data Analysis, Visualization and Electronic Retrieval) http://www.univie.ac.at/cartography/project/wiser/ (Date: 23.02.2015)

Wieloch, T.; Helle, G.; Heinrich, I.; Voigt, M. and Schyma, P. (2011): A novel device for batch-wise isolation of α-cellulose from small-amount wholewood samples. In: Dendrochronologia 29, 115–117. DOI: 10.1016/j.dendro.2010.08.008

Wigley, T.; Briffa, K. R. and Jones, P. D. (1984): On the average value of correlated time series, with applications in dendroclimatology and hydrometeorology. In: Journal of Applied Meteorology and climatology 23, 201–213. DOI:10.1175/1520-0450(1984)023<0201:otavoc>2.0.co;2

Worbes, M. (2002): One hundred years of tree-ring research in the tropics – a brief history and an outlook to future challenges. In: Dendrochronologia 20, 217–231. DOI: 10.1078/1125-7865-00018

Xu, C.; Sano, M. and Nakatsuka, T. (2011): Tree ring cellulose $\delta^{18}O$ of *Fokienia hodginsii* in northern Laos: a promising proxy to reconstruct ENSO? In: Journal of Geophysical Research 116, D24109. DOI: 10.1002/2011JD016694

Xu, C.; Zheng, H.; Nakatsuka, T. and Sano, M. (2013a): Oxygen isotope signatures preserved in tree ring cellulose as a proxy for April–September precipitation in Fujian, the subtropical region of southeast China. In: Journal of Geophysical Research 118, 1–11. DOI: 10.1002/2013JD019803

Xu, C.; Sano, M. and Nakatsuka, T. (2013b): A 400-year record of hydroclimate variability and local ENSO history in northern Southeast Asia inferred from tree-ring $\delta^{18}O$. In: Palaeogeography, Palaeoclimatology, Palaeoecology. DOI: 10.1016/j.palaeo.2013.06.025

Zuidema, P. A.; Baker, P. J.; Groenendijk, P.; Schippers, P.; van der Sleen, P.; Vlam, M. and Sterck, F. (2013): Tropical forests and global change: filling knowledge gaps. In: Trends in Plant Science 18, 413–419. DOI: 10.1016/j.tplants.2013.05.006

Zhu, M.; Stott, L.; Buckley, B.; Yoshimura, K. and Ra, K. (2012): Indo-Pacific warm pool convection and ENSO since 1867 derived from Cambodian pine tree cellulose oxygen isotopes. In: Journal of Geophysical Research 117, D11307. DOI: 10.1029/2011JD017198

Authors

Franziska Volland
Prof. Dr. Achim Bräuning
Friedrich-Alexander-University of Erlangen-Nuremberg
Department of Geography
Wetterkreuz 15
91058 Erlangen
Germany
franziska.volland@fau.de

Darwin Pucha
Universidad Nacional de Loja
Carrera de Ingeniería Forestal
Ciudadela Universitaria Guillermo Falconí Espinosa “La Argelia”
Loja,
Ecuador